Shear Flow and Kelvin-Helmholtz Instability in Superfluids

R. Blaauwgeers,[1] V. B. Eltsov,[1,2] G. Eska,[1,3] A. P. Finne,[1] R. P. Haley,[1,4] M. Krusius,[1] J. J. Ruohio,[1] L. Skrbek,[1,5] and G. E. Volovik[1,6]

[1]*Low Temperature Laboratory, Helsinki University of Technology, P.O. Box 2200, FIN-02015 HUT, Finland*
[2]*Kapitza Institute for Physical Problems, Kosygina 2, 117334 Moscow, Russia*
[3]*Physikalisches Institut, Universität Bayreuth, D-95440 Bayreuth, Germany*
[4]*Department of Physics, Lancaster University, Lancaster LA1 4YB, United Kingdom*
[5]*Joint Low Temperature Laboratory, Institute of Physics ASCR and Charles University, V Holešovičkách 2, 180 00 Prague, Czech Republic*
[6]*Landau Institute for Theoretical Physics, Kosygina 2, 117334 Moscow, Russia*
(Received 3 March 2002; published 20 September 2002)

The first realization of instabilities in the shear flow between two superfluids is examined. The interface separating the *A* and *B* phases of superfluid ^{3}He is magnetically stabilized. With uniform rotation we create a state with discontinuous tangential velocities at the interface, supported by the difference in quantized vorticity in the two phases. This state remains stable and nondissipative to high relative velocities, but finally undergoes an instability when an interfacial mode is excited and some vortices cross the phase boundary. The measured properties of the instability are consistent with the classic Kelvin-Helmholtz theory when modified for two-fluid hydrodynamics.

DOI: 10.1103/PhysRevLett.89.155301 PACS numbers: 67.40.Vs, 47.32.Cc, 67.57.Fg

Instabilities in the shear flow between two layers of fluids [1] belong to a class of interfacial hydrodynamics which is attributed to many natural phenomena. Examples are wave generation by wind blowing over water [2], the flapping of a flag in the wind [3,4], and even flow in granular beds [5]. In the hydrodynamics of inviscid and incompressible fluids the transition from calm to wavy interfaces is known as the Kelvin-Helmholtz (KH) instability [2,6]. Since Kelvin's treatise in 1871, difficulties have plagued its description in ordinary fluids, which are viscous and dissipative. They also display a shear-flow instability, but its correspondence with that in the ideal limit is not straightforward. The tangential velocity discontinuity in the shear flow is created by a vortex sheet. In a viscous fluid a vortex sheet is not a stable equilibrium state and not a solution of the hydrodynamic equations [7].

Superfluids provide a close variation of the ideal inviscid limit considered by Kelvin and thus an environment where the KH theory can be tested. The initial state is a nondissipative vortex sheet—the interface between two superfluids brought into a state of relative shear flow. So far the only experimentally accessible case where this can be studied in stationary conditions is the interface between ^{3}He-*A* and ^{3}He-*B* [8], where the order parameter changes symmetry and magnitude but is continuous on the scale of the superfluid coherence length $\xi \sim 10$ nm. We discuss an experiment, where the two phases slide with respect to each other in a rotating cryostat: ^{3}He-*A* performs solid-body-like rotation while ^{3}He-*B* is in the vortex-free state and thus stationary in the laboratory frame. While increasing the rotation velocity Ω, we record the events when the *AB* phase boundary becomes unstable—when some circulation from the *A* phase crosses the *AB* interface and vortex lines are introduced into the initially vortex-free *B* phase. On increasing the rotation further, the instability occurs repeatedly. Such a succession of instability events can be understood as a spin-up of ^{3}He-*B* by rotating ^{3}He-*A*.

Our experimental setup is shown in Fig. 1. The *AB* boundary is forced against a magnetic barrier in a smooth-walled quartz container, by cooling the sample below T_{AB} at constant pressure in a rotating refrigerator. The number of vortices in both phases is independently determined from the simultaneously measured nuclear magnetic resonance (NMR) spectra [10,11]. The state of the sample can be changed from an all *A* phase to an all *B* phase or to a two-phase configuration. The evolution of the quantized vorticity as a function of Ω is then observed to be radically different when the *AB* interface is present.

The quasi-isotropic ^{3}He-*B* supports singly quantized vortices with a core size comparable to ξ [10]. In the anisotropic ^{3}He-*A* we form vortex lines [11] with continuous Skyrmion topology: Inside its central part the order-parameter amplitude remains constant, but the orientations of the axis of the orbital anisotropy cover a solid angle of 4π. Such a "soft-core" structure carries continuous vorticity with two circulation quanta and is 3 orders of magnitude larger in radius than the "hard" core of the *B*-phase vortex. Thus converting an *A*-phase vortex into a *B*-phase vortex requires a large concentration of the flow energy.

The large difference in core radii is also the origin for the much lower rotation at which vortices start forming in the *A* phase at the outer sample circumference, compared to the *B* phase [10]. If the sample consists of only *B* phase, the critical velocity for forming the first vortex line in the

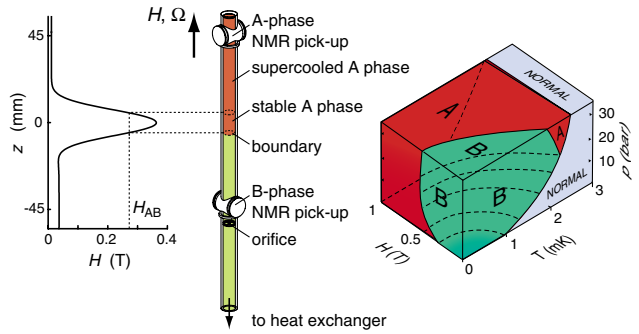

FIG. 1 (color). Stabilization of the first-order ^{3}He-A–^{3}He-B phase boundary. At pressures $p \geq 21$ bars, the A phase extends to lower temperatures in external magnetic field (see phase diagram on the right). The sample (length 11 cm, radius $R = 0.3$ cm) is first cooled to the A phase. On further cooling, the $A \rightarrow B$ transition happens in the coldest place at the bottom. The AB boundary then starts to move up and rises to a height z where the barrier field $H_b(z)$ equals the value of the thermodynamic $A \rightarrow B$ transition $H_{AB}(T, p)$. The A phase in the top section remains in a metastable supercooled state [9]. Ultimately, the boundary disappears when $H_{AB}(T, p) > [H_b(z)]_{max}$. For $p = 29.0$ bars and $H_b(z)$ as shown in the figure with a current of 4 A in the barrier solenoid, the stable AB boundary exists below 2.07 mK down to 1.33 mK. The NMR spectrometers operate in homogeneous static magnetic fields of 10 and 35 mT, chosen for best measuring sensitivity of the single-vortex signal.

setup of Fig. 1 is $v_{cB} > 7$ mm/s [12]. In the A phase the critical velocity v_{cA} is a factor of 20 smaller [13], independently of the presence of the AB boundary.

Vortex lines are thus easily created at low rotation in the A-phase section of the sample, while no vortices are detected in the B-phase section [Fig. 2(a)]. This is the ideal nondissipative initial state where the two superfluid phases slide along each other without friction. When Ω is increased further, sudden bursts of vortex lines are observed in the B-phase section (Fig. 3). The onset Ω_c depends on temperature and on the current in the barrier magnet. Overall, the measured characteristics of the bursts fit a shear-flow instability, which provides a mechanism for the circulation to cross the AB interface.

^{3}He-A and ^{3}He-B are states of the same order-parameter manifold. One of the conditions on their phase boundary is that the phase of the order parameter has to be continuous [14]: If the circulation is not continuing across the interface [Fig. 2(a)] then the existing A-phase vortex lines have to bend and form a vortex layer on the AB interface. This is the only hydrodynamically stable state, with vortex-free flow seen by the B-phase spectrometer and a large cluster of vortex lines detected by the A-phase spectrometer. The buildup of a sheetlike vortex layer means that the A-phase circulation cannot easily penetrate into the vortex-free B phase and the AB interface remains stable up to the measured critical velocity $u_c = \Omega_c R \sim 2$–4 mm/s $< v_{cB}$.

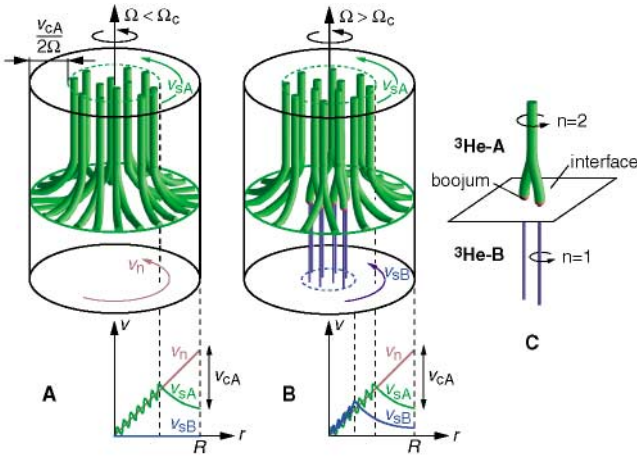

FIG. 2 (color). The two configurations of vortex lines with the AB boundary in rotation. (a) $\Omega < \Omega_c$: Vortex lines are formed in ^{3}He-A while ^{3}He-B remains vortex-free. Near the AB boundary the A-phase vortices bend parallel to the interface and form a vortex sheet between the sliding superfluids. The radial distributions of the normal and superfluid velocities far from the AB interface are depicted below, with $v_{nA} = v_{nB} = \Omega r$, while $v_{sB} = 0$. (b) $\Omega \geq \Omega_c$: Vortices are observed to appear in the B phase in events of a few lines at a time. They form a central cluster in the B-phase section. (c) A hydrodynamically stable state with respect to externally imposed perturbations in Ω, T, or H exists at the AB interface for $\Omega \geq \Omega_c$. A topologically stable configuration for the vortex-line intersection with the AB interface is suggested in Ref. [14]: The doubly quantized A-phase vortex terminates at the AB interface in two point singularities, known as boojums. These, in turn, are the end points of two singly quantized B-phase vortices.

At $\Omega > \Omega_c$, some vortex lines have broken through the AB phase boundary. Thus there exists also a stable configuration in which vortices from the A phase continue into the B phase, where they form a cluster in the center [Fig. 2(b)]. The likely topology of the intersection is illustrated in Fig. 2(c). Thus, although the AB interface is not directly monitored by the two NMR spectrometers, the hydrodynamically stable states below and above Ω_c can only be the configurations in Fig. 2. By comparing B-phase vortex-line creation in the presence and absence of the AB interface, we conclude that the events in Fig. 3 originate from the AB phase boundary.

In the classical KH instability the interface between fluids with densities ρ_1 and ρ_2 becomes destabilized by inertial effects, which are normally balanced by gravity g and surface tension σ. The relative velocity $|v_2 - v_1|$ acts as a drive. When it reaches a critical value [2] given by

$$\frac{\rho_1 \rho_2}{\rho_1 + \rho_2}(v_2 - v_1)^2 = 2\sqrt{\sigma F}, \qquad (1)$$

where $F = g(\rho_1 - \rho_2)$ is the gravitational restoring force, waves with wave vector $k = \sqrt{F/\sigma}$ are created on the interface.

This approach can be generalized for superfluids in terms of two-fluid hydrodynamics [15]. For superfluid

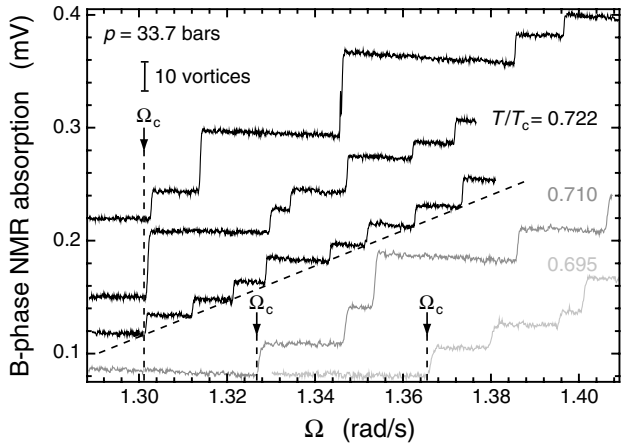

FIG. 3. Instability events during slowly increasing rotation ($d\Omega/dt = 2.5 \times 10^{-4}$ rad/s^2). NMR absorption signals as a function of Ω are recorded (shifted arbitrarily on the vertical scale). The vertical jumps mark events in which δN new vortex lines enter the B phase section of the sample. The height of each jump is proportional to δN, a small stochastic number. When averaged over a large interval of Ω, the number of B-phase vortex lines grows linearly with Ω. This is demonstrated also by the dashed line: the instability occurs independently of Ω at constant critical drive, i.e., $u_c = |v_{sB} - v_n|_{r=R} = \Omega_c R = \text{const}$. The three topmost signal traces were recorded at the same temperature; i.e., measurements at fixed T yield the same Ω_c (if small variations in v_{cA} are accounted for [13]). The two bottom traces at different T illustrate that Ω_c depends on temperature. Here $T_{AB}(H = 0) = 0.785\, T_c$ and H_b as in Fig. 1.

^{3}He under our experimental conditions it is safe to assume that the normal fractions are always in solid-body rotation. Instead of gravity, the restoring force is now produced by the magnetic barrier $H_b(z)$, owing to the difference in the susceptibilities χ_A and $\chi_B(T, H)$: $F = (1/2)[\chi_A - \chi_B(T, H)]\nabla(H_b^2)$ at $H_{AB}(T)$. The restoring force can thus be calculated as a function of temperature and current in the barrier solenoid. The motion of the AB interface with respect to the normal component is subject to a finite damping [16]. Since the initial state is nondissipative, damping modifies, but does not explicitly appear in, the stability condition [17]. The onset of the instability can be derived from the dynamics of small amplitude perturbations, as Eq. (1) is generally derived in textbooks [1], or from the thermodynamics when perturbations of the interface lead to a negative free energy in the rotating frame. The mode for which the interface first becomes unstable has the same wave vector $k = \sqrt{F/\sigma}$ as before at a drive given by

$$\frac{1}{2}\rho_{sA}(v_{sA} - v_n)^2 + \frac{1}{2}\rho_{sB}(v_{sB} - v_n)^2 = \sqrt{\sigma F}, \quad (2)$$

where ρ_s, ρ_n and v_s, v_n are the densities and velocities of superfluid and normal components.

In Fig. 4 we plot the measured $\Omega_c(T)$ for the magnetic barrier profiles $H_b(z)$ at three different constant solenoid currents. To compare with Eq. (2) we note that the maximum of $|v_{sA} - v_n|$ in the A phase is limited by the small critical velocity v_{cA} [13]: in practice we may set $v_{sA} - v_n \approx 0$. As seen in the figure, with no fitting parameters the agreement with experiment is surprisingly good. We may also compare with the classical formulation in Eq. (1) by setting $|v_1 - v_2| = |v_{sA}(R) - v_{sB}(R)| = R\Omega_c$, and $\rho_1 = \rho_2 = \rho_s(T, H)$. We then find that this critical velocity is by $\approx \sqrt{2}$ larger than that from Eq. (2) and the fit to measurements not as good.

In the classical expression (1) only the relative velocity matters while in two-fluid hydrodynamics reference frame considerations are important. In Eq. (2) the reference frame is fixed to the rotating container. Here it is the "superfluid winds"—the counterflow of the superfluid and normal components, $|v_s - v_n|$, on each side of the interface—which produce the instability. It takes place even if the two superfluids have the same densities and velocities. In this sense it resembles the flapping flag instability discussed by Rayleigh [3] where the fixed reference frame is provided by the flagpole. In the superfluid it is the normal components of both phases which establish the contact between the superfluid fractions and the container walls. After a change in Ω, ultimately at constant Ω the normal components achieve solid-body rotation with the container. Therefore Eq. (2) should

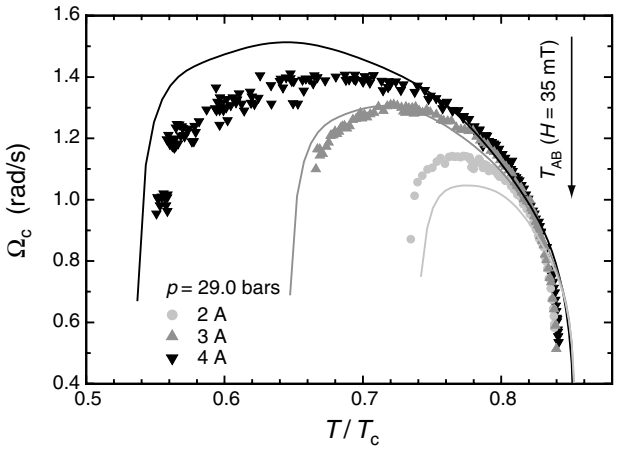

FIG. 4. Critical velocity Ω_c for the first appearance of B-phase vortex lines in the presence of the AB boundary as a function of temperature, while Ω is slowly increased ($\dot{\Omega} = 5 \times 10^{-4}$ rad/s^2). The current in the barrier solenoid is constant but different for the three sets of data. It controls the magnetic force F which is largely responsible for the shape of the curves: As a function of decreasing temperature the curves start at $T_{AB}(H_{AB} = 35$ mT) and end at the temperature at which H_{AB} equals the maximum value of the barrier field H_b at the given current. The steep slopes at both ends of the curves are caused by the rapidly changing value of ∇H_b. The solid curves represent Eq. (2) if one sets $\Omega_c = |v_{sB} - v_n|/R$ and $v_{sA} = v_n$. No fitting parameters are used. The values for $\sigma(T)$, $\chi_A - \chi_B(T, H)$, and $\rho_{sB}(T, H)$ are obtained from accepted references [8,18–20], while H_b and ∇H_b apply for the profile $H_b(z)$ at the location of the AB boundary: $H_{AB}(T) = H_b(z)$.

remain valid even in the low temperature limit, when $\rho_n \to 0$ and $\rho_{sA} \approx \rho_{sB} \to \rho$, if one waits long enough.

A further comparison to Eq. (2) is obtained from the number δN of new B-phase vortex lines after an instability event. In Fig. 3 it is seen that $\delta N \approx 10$. At $0.77\,T_c$ (with $u_c = \Omega_c R = 0.39$ cm/s at 29.0 bars) the measured average for more than 100 events is $\delta N = 11$. We interpret δN to correspond to the number of circulation quanta $\kappa = h/2m_3$, which fit in one corrugation of the interface mode of size $\lambda_c/2 = \pi/k$. If we set $v_{cA} \approx 0$, then there are in solid-body rotation $N \approx \pi R^2 \Omega_c/\kappa$ vortex lines in the A phase which all flare out into the lateral sample boundary at the AB interface [Fig. 2(a)]. Measured along the perimeter of the sample there are $\Omega_c R/\kappa$ circulation quanta per unit length and thus in one corrugation $\delta N \approx (\pi u_c)/(k\kappa)$. From Eq. (2) this is seen to be $\delta N \approx (2\pi\sigma)/(\kappa u_c \rho_{sB})$, which at $0.77\,T_c$ gives nine vortex lines in agreement with the measured number.

Earlier rotating experiments have all been performed in the absence of a strong magnetic field gradient. It is then not possible to localize the AB interface at a fixed position. Instead one can record the motion of the interface through the sample in a slow $A \to B$ transition during cooling at constant Ω [21]. An A-phase vortex layer and tangential vortex-free B-phase counterflow are moving with the interface. Depending on the interface velocity, part of the A-phase vortex lines are swept with the interface to the sample boundary and are annihilated there, while part of the lines break through the boundary into the B phase. As a result the total circulation is found to be reduced after the $A \to B$ transition. As the AB interface is in motion, the state is dissipative and Eq. (2) is not directly applicable. Nevertheless, applying dimensional arguments we find that the time for the KH instability to develop is $\sim(ku_c)^{-1}$, which from Eq. (2) is seen to be $\sim\sigma/(u_c^3\rho_{sB})$. To form vortices, this time must be less than the transition time t_{AB} for the $A \to B$ interface to sweep through the entire sample. This leads to an effective critical velocity $u_c \sim [\sigma/(\rho_{sB} t_{AB})]^{1/3}$. It fits the measurements in Ref. [21] in the limit of slow interface velocities and shows that the AB interface becomes stiffer and less permeable at increasing velocity. At suitable velocities the removal of vortices from the system in front of the moving AB phase boundary becomes quite effective. Similar mechanisms have been discussed for sweeping away the abundantly created magnetic monopoles from the early Universe [22].

To summarize, in uniform rotation the magnetically stabilized AB phase boundary has been found to give rise to a state with tangential superfluid shear flow. The reason for this is a large energy barrier which prevents the nucleation of point and line defects on the small length scale ξ. This situation evolves into the first example of a shear-flow instability where the initial state is nondissipative. The outcome of the instability is the transmission of a burst of vorticity across the interface. The instability creates corrugations in the interface and its vortex coating, upon which the vortex lines in the deepest trough are pulled by the Magnus force through the boundary. The process represents a new intrinsic mechanism of defect formation, applicable to interfaces between superfluids or to the free surface of a superfluid [23].

This collaboration was carried out under the EU-IHP program ULTI 3 and the ESF program COSLAB.

[1] H. Lamb, *Hydrodynamics* (Dover, New York, 1932), Chap. IX; L. D. Landau and E. M. Lifshitz, *Fluid Mechanics* (Pergamon Press, New York, 1989), Chap. VII.
[2] Lord Kelvin (Sir William Thomson), *Hydrodynamics and General Dynamics*, Mathematical and Physical Papers Vol. 4 (Cambridge University Press, Cambridge, England, 1910).
[3] Lord Rayleigh (J.W. Strutt), *Scientific Papers* (Cambridge University Press, Cambridge, England, 1899).
[4] J. Zhang *et al.*, Nature (London) **408**, 835 (2000).
[5] D. J. Goldfarb *et al.*, Nature (London) **415**, 302 (2002).
[6] H. L. F. von Helmholtz, Monatsberichte der königlichen Akademie der Wissenschaften zu Berlin vom April, 215 (1868).
[7] G. Birkhoff, in *Hydrodynamic Instability*, Proc. Symp. Appl. Mathematics Vol. XIII, edited by G. Birkhoff, R. Bellman, and C. Lin (American Mathematical Society, Providence, 1962), p. 55.
[8] D. Vollhardt and P. Wölfle, *The Superfluid Phases of ^3He* (Taylor & Francis, London, 1990).
[9] P. Schiffer and D. Osheroff, Rev. Mod. Phys. **67**, 491 (1995).
[10] Ü. Parts *et al.*, Europhys. Lett. **31**, 449 (1995); J. Low Temp. Phys. **107**, 93 (1997).
[11] R. Blaauwgeers *et al.*, Nature (London) **404**, 471 (2000).
[12] With only B phase in the sample, v_{cB} is determined by single-vortex formation at the sample boundary or by the leakage of vortices through the bottom orifice. Both processes differ in appearance from the events in Fig. 3.
[13] In this experiment the A-phase critical velocity is $v_{cA} \approx (0.36 \pm 0.06)$ mm/s.
[14] G. E. Volovik, Physica (Amsterdam) **178B**, 160 (1992).
[15] D. R. Tilley and J. Tilley, *Superfluidity and Superconductivity* (IOP, Bristol, 1990).
[16] D.S. Buchanan *et al.*, Phys. Rev. Lett. **57**, 341 (1986).
[17] G.E. Volovik, Pis'ma Zh. Eksp. Teor. Fiz. **75**, 491 (2002) [JETP Lett. **75**, 418 (2002)].
[18] D. Osheroff and M. Cross, Phys. Rev. Lett. **38**, 905 (1977).
[19] J. C. Wheatley, Rev. Mod. Phys. **47**, 415 (1975).
[20] Y. H. Tang *et al.*, Phys. Rev. Lett. **67**, 1775 (1991).
[21] M. Krusius, E.V. Thuneberg, and Ü. Parts, Physica (Amsterdam) **197B**, 376 (1994); Phys. Rev. Lett. **71**, 2951 (1993).
[22] G. Dvali *et al.*, Phys. Rev. Lett. **80**, 2281 (1998).
[23] S.E. Korshunov, Pis'ma Zh. Eksp. Teor. Fiz. **75**, 496 (2002) [JETP Lett. **75**, 423 (2002)].